Acute Intracranial Hemorrhage: Intensity Changes on Sequential MR Scans at 0.5 T

Robert D. Zimmerman[1]
Linda A. Heier[1]
Robert B. Snow[2]
David P. C. Liu[1]
Anna B. Kelly[1]
Michael D. F. Deck[1]

Thirty-seven patients underwent MR imaging at 0.5 T within 7 days of a CT-documented intracranial hemorrhage. A total of 57 hematomas were evaluated. Twelve patients underwent serial scanning and 12 patients had multiple hemorrhages into different intracranial compartments. The appearances of the hematomas on spin-echo (SE) images with a short repetition time (TR) of 500 msec and short echo time (TE) of 32 msec (SE 500/32), long TR/intermediate TE (SE 2000/60), and long TR/long TE (SE 2000/120) were carefully evaluated with specific attention to the precise time after ictus. Hematomas showed heterogeneous, complex, rapidly changing intensities. There was a significant amount of variation among patients, especially between the third and seventh days. Hematomas studied between 12 and 24 hr after hemorrhage were mildly hyperintense on short TR scans and markedly hyperintense on long TR (intermediate and long TE) scans (stage I). These findings in acute hemorrhage have received little prior attention. Over the next 1–2 days, hematomas became iso- to mildly hypointense on short TR scans and markedly hypointense on long TR scans (stage II). Hypointensity on long TR scans has previously been described at high field strengths; our communication demonstrates that this phenomenon is seen routinely at intermediate field strengths as well. Hematomas became markedly hyperintense on short TR scans beginning on approximately the fourth day postictus and redeveloped hyperintensity on long TR scans approximately 5–6 days after ictus (stage III). By the end of the first week they were hyperintense on all pulse sequences (stage IV).

MR findings on the first day after intracranial hemorrhage (in particular, subtle hyperintensity on short TR scans) probably allow for a specific diagnosis, while the variable, heterogeneous, and rapidly changing intensities noted between days 2 and 7 are often less specific.

This article appears in the January/February 1988 issue of *AJNR* and the March 1988 issue of *AJR*

Received March 13, 1987; accepted after revision August 12, 1987.

Presented at the annual meeting of the American Society of Neuroradiology, San Diego, January 1986, and presented in part at the Symposium Neuroradiologicum, Stockholm, June 1986.

[1] Department of Radiology, New York Hospital–Cornell University Medical Center, 525 E. 68th St., New York, NY 10021. Address reprint requests to R. D. Zimmerman.

[2] Department of Neurosurgery, New York Hospital–Cornell University Medical Center, New York, NY 10021.

***AJR* 150:651–661, March 1988**
0361–803X/88/1503–0651

The MR appearance of intracranial hemorrhage has been the subject of many communications. Findings in acute hemorrhage, particularly within 48 hr of ictus, remain controversial and incompletely delineated [1–9]. The intensity of hematomas is known to be dependent on multiple factors including time from ictus and pulse sequence employed [1, 6, 7]. Recently, it has been suggested that the field strength of the MR imager may also affect intensity such that "acute" (under 7 days) hemorrhage may be detected more easily at ultralow (0.02 T) [4] or high (1.5 T) field strengths [5] than at intermediate field strengths (0.1–0.6 T). Unfortunately, all prior studies of acute hemorrhage are limited by the small number of patients evaluated in each series. Extrapolations from these limited data have led to confusing and often contradictory conclusions. To clarify the findings in acute hemorrhage on MR, we studied 37 patients within 1 week of an acute hemorrhagic ictus with specific attention to the precise relationship between the intensity of the lesion and the time from ictus. The implications of these findings on previously presented theories of hematoma intensity will be discussed, as will the efficacy of MR and CT in the clinical evaluation of patients with suspected acute intracranial hemorrhage (AIH).

TABLE 1: Relationship Between Time After Ictus and Cause and Location of Hemorrhage

Cause/Location	No. by Day							Total
	1	2	3	4	5	6	7	
Cause:								
Trauma	0	2	3	6	2	3	5	21
Hypertension	1	2	2	1	1	0	0	7
Vascular[a]	1	1	0	0	0	2	1	5
Neoplasm	0	1	0	1	0	0	0	2
Idiopathic/miscellaneous[b]	0	1	0	1	1	1	4	8
Location of hematoma:								
Epidural	0	0	1	1	0	2	0	4
Subdural	1	1	1	5	2	1	5	16
Parenchymal	2	6	3	5	2	4	6	28
Subarachnoid	0	2	0	1	0	1	1	5
Intraventricular	1	2	1	0	0	0	0	4
Total	4	11	6	12	4	8	12	57

[a] Includes aneurysms, arteriovenous malformations, and venous angiomas.
[b] Includes hemorrhage without known cause, venous thrombosis, and amyloid angiopathy.

Subjects and Methods

Thirty-seven patients were included in this study. In each case, a CT-documented hemorrhage had occurred within 1 week of the initial MR. The time from clinical ictus to MR imaging was identified as precisely as possible, as were the cause and location of the hemorrhage (Table 1). All patients were evaluated on a 0.5-T MR imaging device.* When hematomas in multiple compartments (12 cases) were present, these were evaluated separately, since they often had different intensities (see Results). Serial studies (12 cases) were also evaluated individually and included within the overall tabulation. Thus, the total number of hematomas evaluated (57) exceeded the number of patients (37). T1-weighted spin-echo (SE) images with a short repetition time (TR) of 500 msec and short echo time (TE) of 32 msec (SE 500/32) were obtained in all cases. Moderately T2-weighted long TR/intermediate TE (SE 1500/90) single-echo images were obtained in the initial six patients, while the remaining 31 patients had multiecho scans with a TR of 2000 msec and two echoes (TE = 60–120 msec) or four echoes (TE = 30–120 msec). These scans were subdivided into long TR/intermediate TE images (for example, SE 2000/60), in which spinal fluid was gray, and long TR/long TE images (for example, SE 2000/120), in which spinal fluid was white. The intensity of the hemorrhages was qualitatively compared with that of white matter on all images. More precise quantitative measurements were not attempted, because hematomas showed quite heterogeneous intensities. The MR findings on each pulse sequence were compared with each other and with CT findings to determine the relative clinical efficacy of each pulse sequence and of MR, in general, when compared with CT in the evaluation of AIH.

Results

Hematomas undergo rapid, reversible changes in intensity that vary with the pulse sequences used. Therefore, relationships between time and intensity for each pulse sequence have been tabulated and are presented in graphic form (Fig. 1). The effects of two additional factors, recurrent hemorrhage and site of hemorrhage, were also evaluated.

* Technicare.

Short TR/Short TE Images

Hematomas evaluated 12–24 hr after an acute ictus (Fig. 2) were subtly and uniformly hyperintense relative to white matter in three examples of AIH (Figs. 2C and 2D) and isointense in one case. The average intensity of AIH diminished over the next 2 days (Fig. 1). Appropriately timed serial studies were not performed in any of these patients and, therefore, the diminishing intensity could not be demonstrated directly. Lesions studied at 24–48 hr had variable intensity, ranging from mild hypo- to mild hyperintensity (Fig. 3). The two hematomas that were hyperintense were evaluated early on the second day (30 and 32 hr, respectively). Hematomas studied on the third to fourth postictal day (Figs. 3–5) demonstrated the greatest variation; mild hyperintensity was the most commonly encountered pattern (Figs. 4C and 5B). Features were similar to those seen on day 1, except that small foci of more marked hyperintensity were often seen within these older hematomas (Fig. 3G). Thereafter, there was a dramatic and progressive increase in intensity (Fig. 6B), which was most prominent near the periphery of the hematoma. This phenomenon was directly observed in five patients studied serially within the first week of ictus (Figs. 4E and 5E) and in another four patients in whom follow-up examinations were performed after 1 week (10–28 days).

Long TR/Intermediate to Long TE Images

Hematomas evaluated within 24 hr of ictus were typically hyperintense (Figs. 2E–2H); hypointensity was present in only one case studied at 24 hr. Thereafter, there was a dramatic decrease in intensity. Hypointensity was present in seven of 11 hemorrhages evaluated during the second postictal day (Fig. 1). The four hematomas without hypointensity were in two patients with multiple hemorrhages evaluated before 36 hr. On the third postictal day, hypointensity was seen in five of six hematomas, and the hypointense components were larger and/or darker than those seen on day 2 (Fig. 4D). The

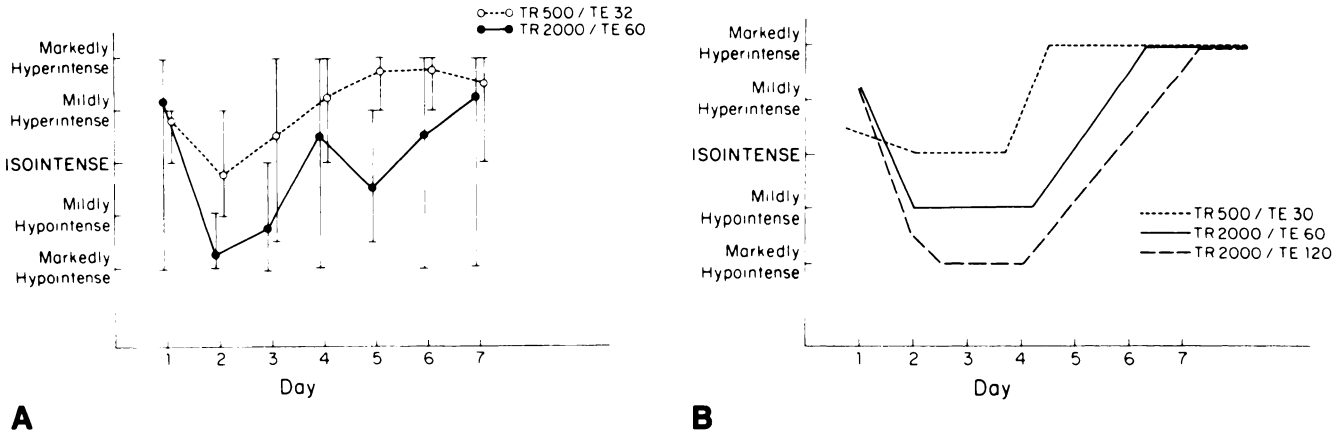

Fig. 1.—Time/intensity curves for acute intracranial hemorrhage.

***A*, All hematomas are plotted. Intensity on each day is given relative to white matter. Range of intensities is shown by vertical bars and mean intensities for all hematomas on each day are *open circles* (TR = 500 msec, TE = 32 msec) or *solid circles* (TR = 2000 msec, TE = 60 msec).**

***B*, Mean intensities only are plotted for SE 500/32 and SE 2000/60–120 scans. Cases in which multiple episodes of hemorrhage were present have been eliminated to simplify curves.**

development of hypointensity from days 1 to 3 was observed directly in four hematomas studied serially during this period (Figs. 3E and 3H). From days 4–7, there was a trend toward increasing intensity, but AIHs studied during this period showed the greatest variation in intensity on long TR images (Figs. 4 and 6).

Comparison of Pulse Sequences

There was poor correspondence between short and long TR scans. The intensities encountered within individual hematomas were different, as was the degree of heterogeneity (Fig. 4). The timing and rate of change of intensity reversals were also different (note the differences in the slopes of the time/intensity curves in Fig. 1B). By contrast, hematomas had similar appearances on long TR/intermediate TE and long TR/long TE scans; the only discernible difference was accentuation of hypointensity on the long TE sequence (Figs. 5C and 5D).

Additional Factors That Affect AIH Intensity

The AIHs in 12 patients with CT and/or clinical evidence of multiple episodes of hemorrhages were more heterogeneous in appearance and more likely to vary from "typical" intensities than those encountered in patients with single hemorrhagic events (Fig. 4). The effect of hematoma location was analyzed by evaluating the patients with hemorrhages into multiple intracranial compartments. In nine of 12 cases, intensity differences were observed. The greatest differences occurred in patients in whom extraaxial or parenchymal hematomas were combined with hemorrhages into spinal fluid compartments (Fig. 3). In patients with simultaneous extraaxial and parenchymal hematomas, the intensities tended to be similar (Fig. 2).

Discussion

The MR features of AIH are complex, fascinating, and incompletely understood. Different investigators have reported a variety of findings and have come to often contradictory conclusions about the physical basis of these phenomena and their clinical implications [1–9]. In our judgment, this confusion and contradiction arise from attempts to extrapolate general principles from very limited clinical and/or experimental data. This type of analysis worked well with CT, in which the densities of hematomas are relatively uniform and change slowly [10, 11]. However, the intensity patterns and shifts that occur with MR are much more complex. Hematoma intensity is typically heterogeneous, and changes rapidly and continuously during the first postictal week. Findings in our series indicate that these shifts are bidirectional (AIH decreasing and then increasing in intensity) and subject to significant variation among patients. Thus, general conclusions drawn from limited clinical experience have proved to be incorrect or, at least, incomplete. Previous attempts to reconcile contradictory findings have centered on the effects of extrinsic, equipment-dependent factors, such as variations in pulse sequences and, more recently, the field strength of the MR imager [4, 5]. Although these factors are undoubtedly important, their true contributions remain unclear. Data from our series indicate that at least some of the apparent discrepancies disappear when a large number of cases are analyzed with careful attention to both the precise time after ictus and the exact intensities encountered. These data also make it possible to gain a firmer understanding of the underlying biochemical changes that produce these alterations in intensity and to delineate four stages in AIH evolution, each with a typical pattern of intensity on multiple pulse sequences.

On short TR/short TE scans, AIH is hyperintense relative to brain when studied between 15 and 24 hr (Fig. 2). The initial mild hyperintensity is unexpected, since most authors report that hematomas are iso- to hypointense relative to

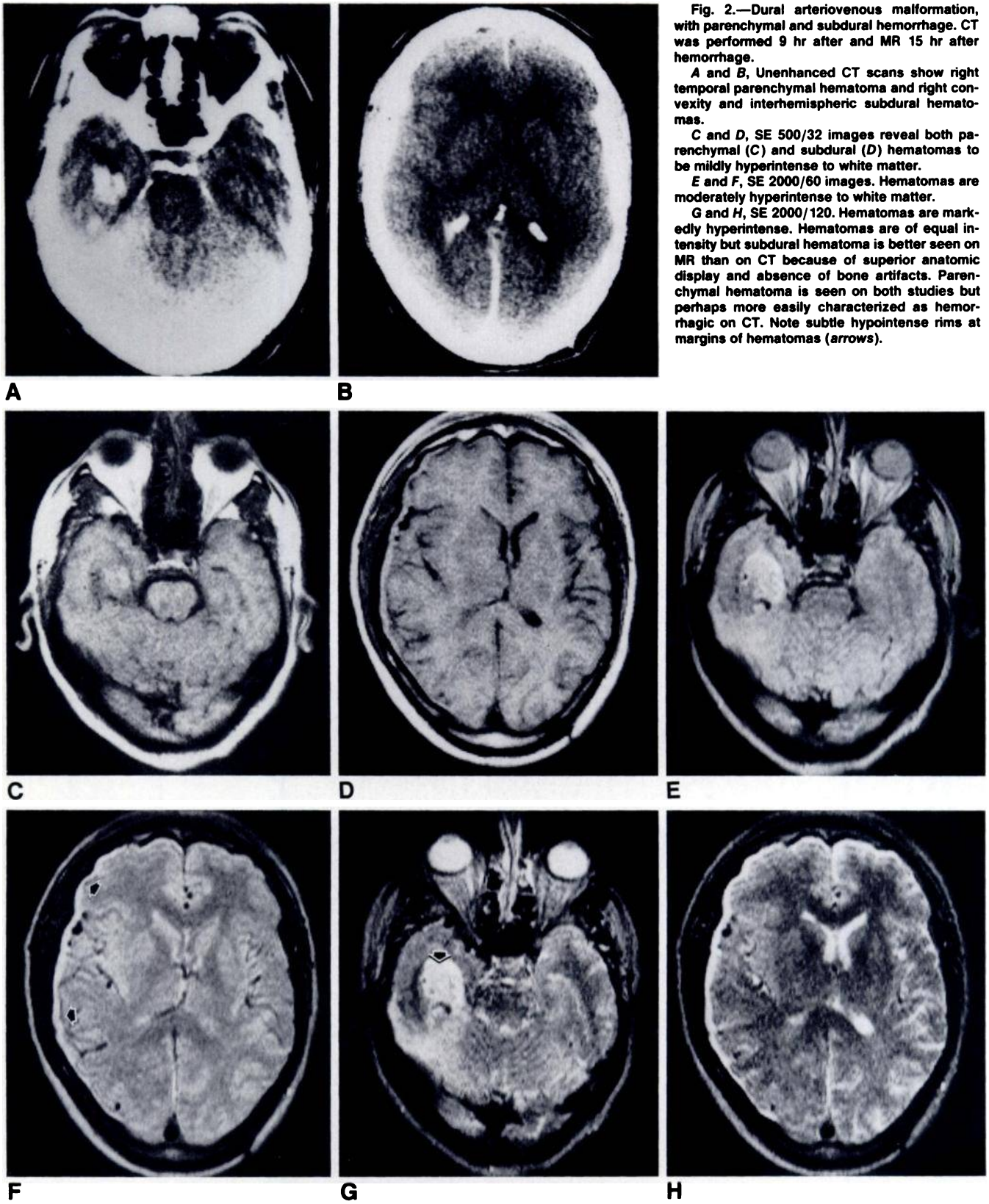

Fig. 2.—Dural arteriovenous malformation, with parenchymal and subdural hemorrhage. CT was performed 9 hr after and MR 15 hr after hemorrhage.

***A* and *B*, Unenhanced CT scans show right temporal parenchymal hematoma and right convexity and interhemispheric subdural hematomas.**

***C* and *D*, SE 500/32 images reveal both parenchymal (C) and subdural (*D*) hematomas to be mildly hyperintense to white matter.**

***E* and *F*, SE 2000/60 images. Hematomas are moderately hyperintense to white matter.**

***G* and *H*, SE 2000/120. Hematomas are markedly hyperintense. Hematomas are of equal intensity but subdural hematoma is better seen on MR than on CT because of superior anatomic display and absence of bone artifacts. Parenchymal hematoma is seen on both studies but perhaps more easily characterized as hemorrhagic on CT. Note subtle hypointense rims at margins of hematomas (*arrows*).**

Fig. 3.—Traumatic epidural and subarachnoid hematomas.

***A* and *B*, CT scans at 21 hr after trauma show hyperdense frontal epidural hematoma and focal left suprasellar subarachnoid hematoma (*A*).**

***C*, SE 500/32 scan at 36 hr. Epidural hematoma is isointense to brain but easily detected; subarachnoid hematoma cannot be seen (nor was it seen on long TR images at this time).**

***D* and *E*, SE 2000/30 (proton-density) (*D*) and SE 2000/90 (heavily T2-weighted) (*E*) scans at 36 hr. Epidural hematoma is hyperintense to brain. Nodules of hypointensity are seen within epidural and subgaleal hematomas.**

***F* and *G*, SE 500/32 scans at 72 hr. Subarachnoid hematoma is now hyperintense to white matter (*F*); epidural hematoma (*G*) is now mildly hypointense to white matter; medial hypointense rim (*G*) represents displaced dura (*arrow*). Epidural hematoma is well seen despite lack of contrast due to improved anatomic display.**

***H*, SE 2000/60 scan at 72 hr. Epidural and subgaleal hematomas have become markedly hypointense to white matter (compare with *E*).**

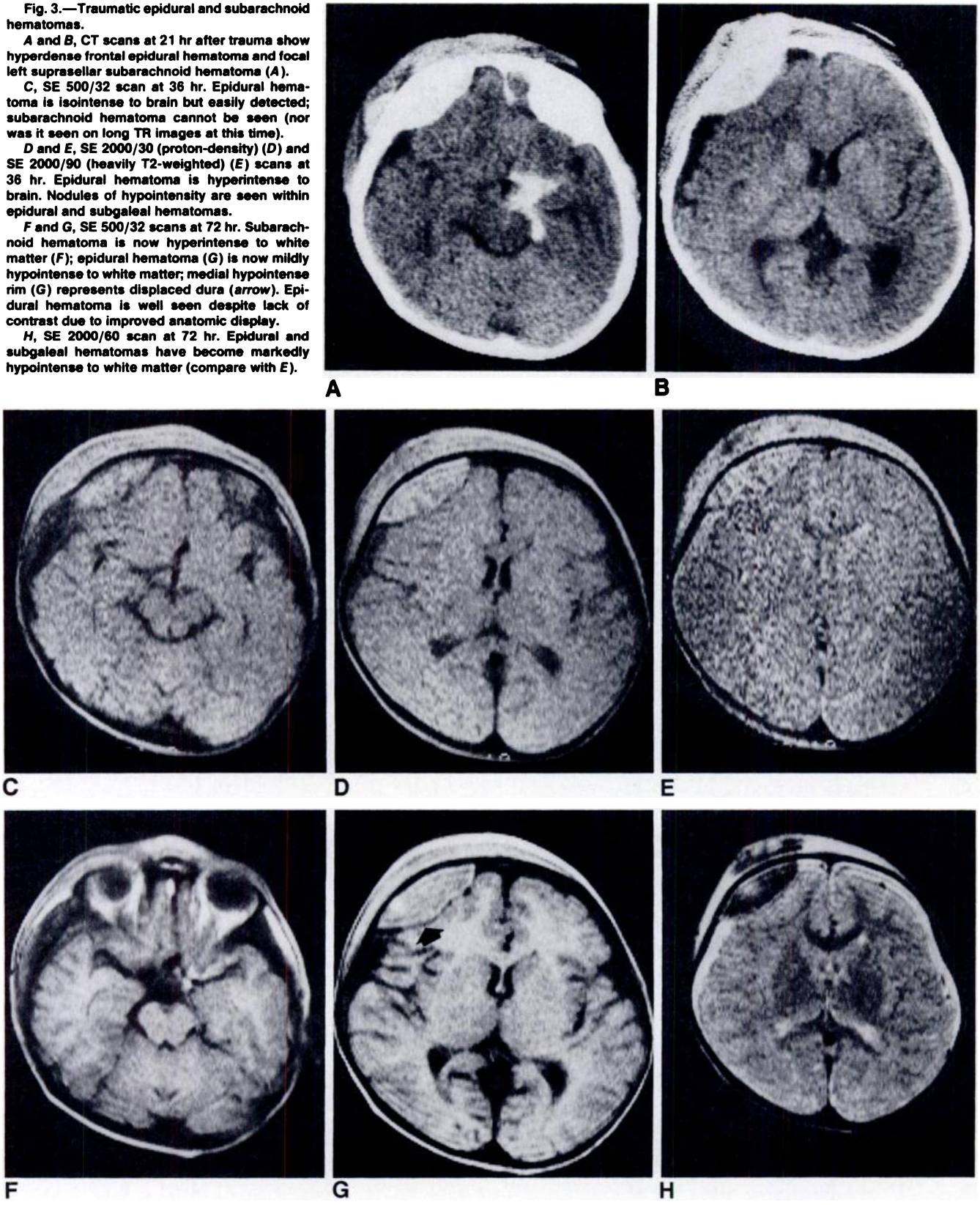

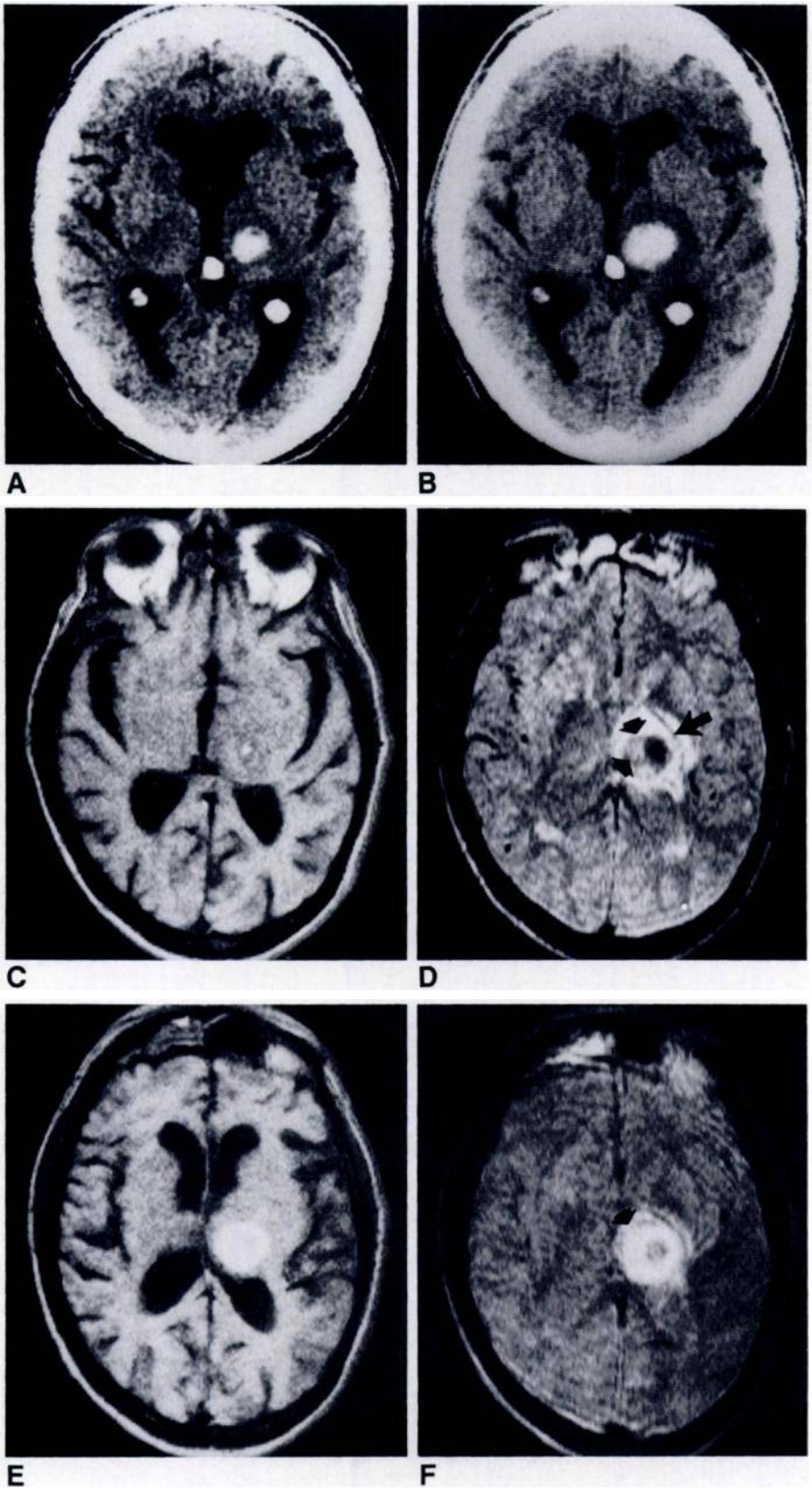

Fig. 4.—Recurrent hypertensive thalamic hemorrhage.

***A*, Initial CT scan 24 hr after initial ictus shows left thalamic hematoma.**

***B*, Follow-up study 1 day later because of increasing drowsiness shows recurrent hemorrhage with enlargement of hematoma.**

***C*, SE 500/32 scan 72 hr after initial hemorrhage. Lesion is predominantly hypointense with small central focus of hyperintensity.**

***D*, SE 2000/60 scan at the same time. Eccentric hypointense focus is noted in lateral aspect of hematoma. Curvilinear hypointensity is also noted within and at margin of hematoma (*short arrows*). More laterally placed linear hypointensity corresponds to internal capsule (*long arrow*).**

***E*, SE 500/32 scan at 6 days. Hematoma is diffusely hyperintense.**

***F*, SE 2000/60 scan at 6 days. Lesion is predominantly hyperintense with small focus of hypointensity near center of hematoma. Hypointense rim marks edge of hematoma (*arrow*).**

Fig. 5.—Hypertensive lenticular nucleus hematoma.

***A*, CT scan at 24 hr.**

***B*, SE 500/32 scan at 72 hr. Lesion is isointense to white matter.**

***C* and *D*, SE 2000/60 (*C*) and SE 2000/120 (*D*) images at 72 hr. Nodular hypointense focus at center of hematoma is surrounded by hyperintensity. Since hypointense focus is smaller than hematoma seen on CT, peripheral hyperintensity represents combination of both hemorrhage and edema.**

***E–G*, Follow-up MR scans at 7 days. Hematoma is diffusely hypointense on all sequences. Thin peripheral rim is seen at margin of lesion on SE 2000/60 (*F*) and SE 2000/120 (*G*) scans.**

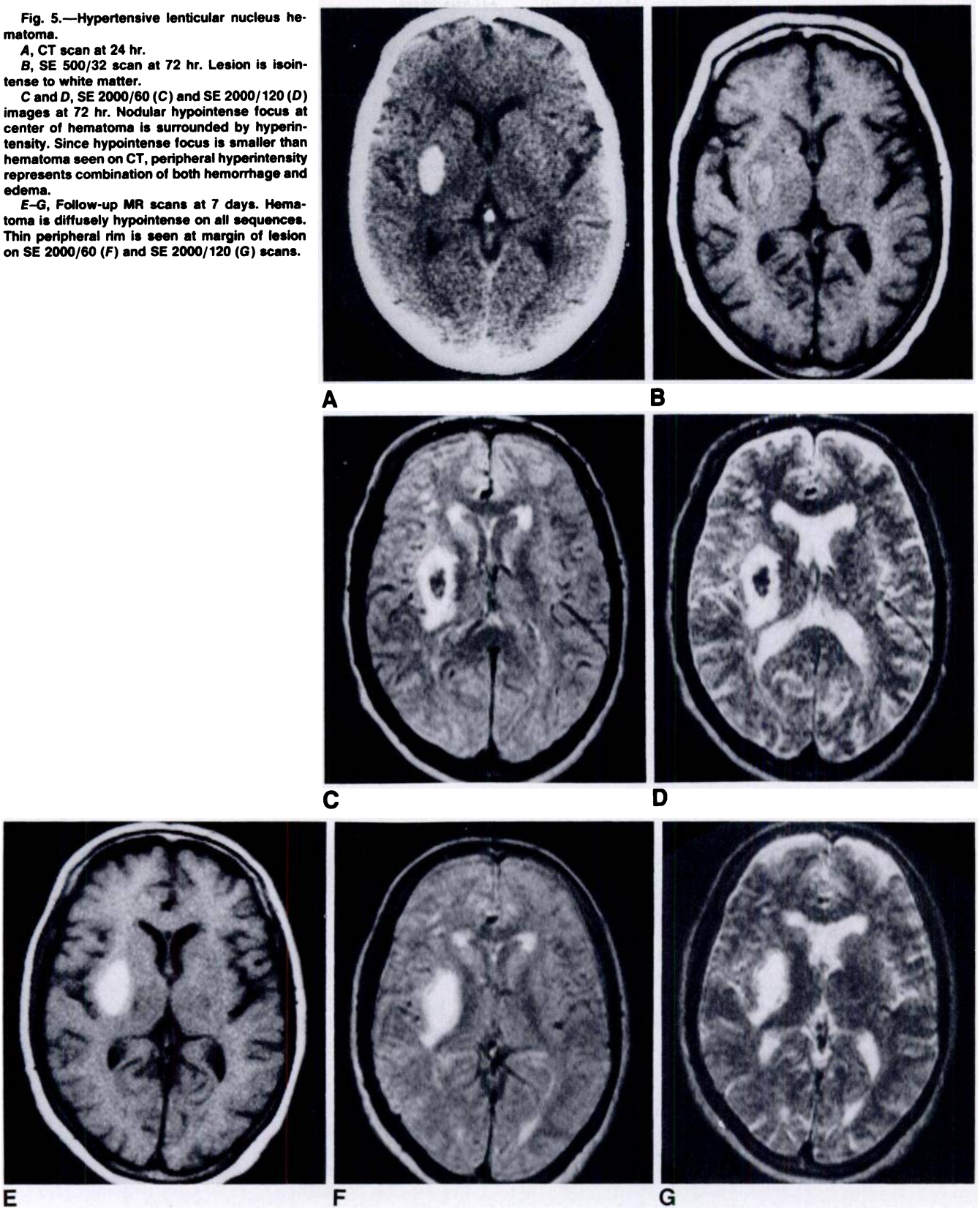

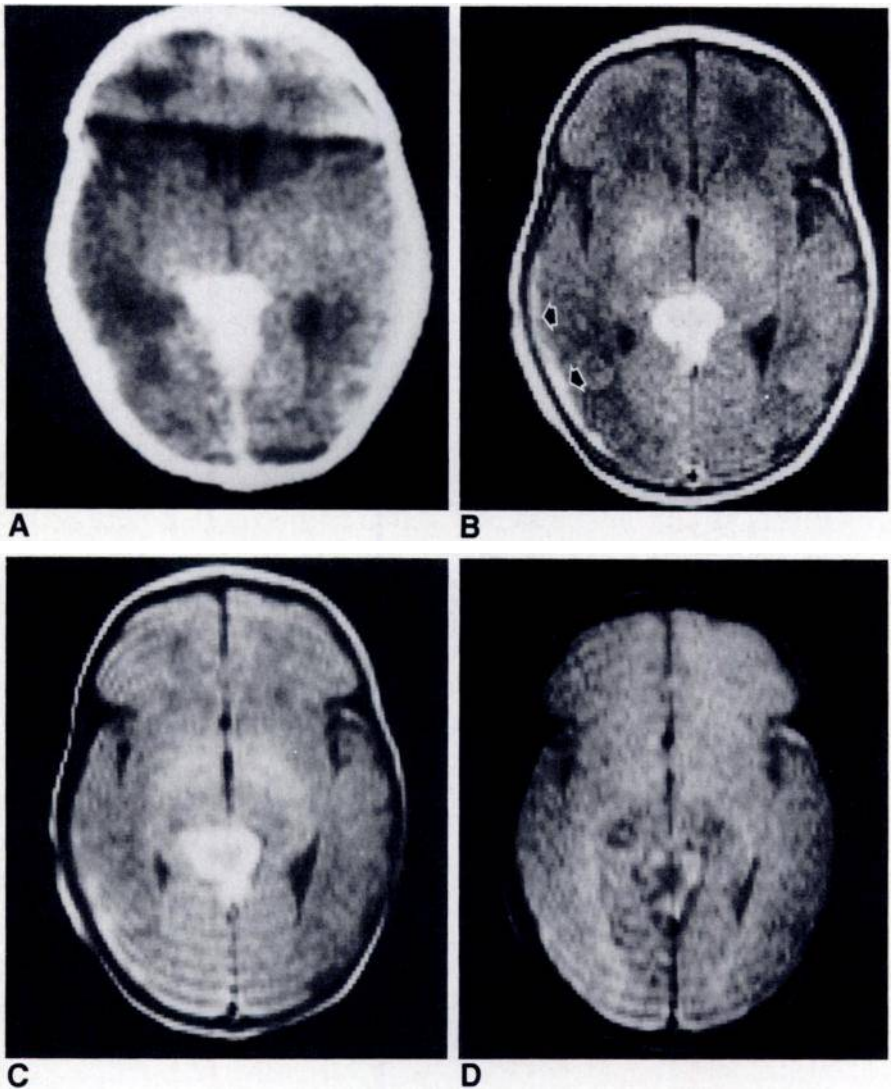

Fig. 6.—Birth trauma with retro-third ventricular subarachnoid and subdural hematoma.

***A*, CT scan 3 days after birth. Subarachnoid hematoma is noted behind third ventricle.**

***B*, SE 500/32 image 6 days after birth. Retro-third ventricular hematoma is hyperintense. Small-convexity hematoma (*arrows*) could not be seen on CT.**

***C* and *D*, SE 2000/60 (*C*) and SE 2000/120 (*D*) images 6 days after birth. Hematoma becomes progressively less intense and mimics intensity of subcutaneous and intraorbital fat. Thus, retroventricular lesion could be confused with congenital midline fat-containing lesion.**

brain throughout this period [2, 5–7]. Careful review of published images, however, reveals subtle diffuse or focal hyperintensity within hematomas that are generally characterized as isointense (see Fig. 1B of Dooms et al. [7]). The underlying basis of this finding is unclear. Hyperintensity on short TR/short TE scans usually results from T1 shortening (relative to adjacent brain), and yet in vivo [1, 7, 12] and in vitro [12, 13] calculations indicate that T1 is initially prolonged relative to white matter. It seems likely, therefore, that the subtle hyperintensity initially encountered on short TR/short TE scans is related to changes in other MR parameters. Since T2 prolongation does not generally produce hyperintensity on short TR/short TE scans [14, 15], high proton density must be considered the probable cause of this phenomenon. Hyperintensity caused by high proton density may be directly observed on an SE 2000/30 ("proton-density") scan (Fig. 3D). The high proton density of acute extravasated blood is probably a reflection of the high water content of liquid blood before clot formation and retraction.

Over the next day, the mean intensity diminishes, and by the end of the second day, hematomas are iso- to hypointense relative to brain (Fig. 3). This decrease in intensity (compare Figs. 2 and 3) may be from T1 prolongation. An alternate explanation, however, is that the T2 shortening that occurs during this period (see below) may be of sufficient magnitude to diminish intensity on these so-called T1-weighted short TR scans in which the TE is 32 msec.

Between the third and fifth days after hemorrhage, the intensity on short TR/short TE scans dramatically and abruptly increases so that hematomas become markedly hyperintense (more prominently at the periphery than at the center of the AIH) in as little as 24 hr (Figs. 4–6). This phenomenon has been demonstrated in previous reports [1–8] and is believed to be secondary to a paramagnetic effect of the oxidative breakdown product methemoglobin, which begins to appear on about the third posthemorrhage day [16, 17]. By the end of the first week, all hematomas show marked hyperintensity on short TR/short TE scans.

On long TR scans, hematomas are more heterogeneous and show greater variation in intensity than on short TR scans. The lesions are generally hyperintense relative to brain when evaluated 12–24 hr after ictus (Fig. 2). Small nodules of hypointensity may be identified within the AIH, and a peripheral rim of hypointensity is commonly seen (Fig. 2). More generalized hypointensity, of variable degree and occupying a variable amount of the hematoma (as identified by CT), develops late in the first or early in the second postictal day and becomes most marked by the third to fourth postictal day (Figs. 3–5).

The inital hyperintensity and early conversion to hypointensity were seen directly in serial studies in two of our patients (Fig. 3) and in one published example [18]. These serial changes were documented in an experimental hematoma studied by Di Chiro et al. at 0.6 T [12]. The early hyperintensity on long TR scans is indicative of T2 prolongation relative to normal brain. Whether this is a property of normal, nonflowing blood or represents some early postextravasation biochemical change is not known, but it is probably related to the fact that, as a fluid, blood has a higher water content and thus a longer T2 than normal brain tissue does. The subsequent development of hypointensity is indicative of T2 shortening. This phenomenon was initially described by Gomori et al. [5], who postulated that it was a paramagnetic effect of the deoxyhemoglobin within intact hypoxic RBCs. Paramagnetic T1 shortening does not occur with deoxyhemoglobin despite the presence of four unpaired electrons, because its molecular structure does not allow the proximity (3 Å) of unpaired electrons necessary to produce T1 shortening [19]. Before cell lysis, however, the deoxyhemoglobin may produce T2 shortening because of its effect on magnetic susceptibility (the ratio between external applied magnetic field and the internal field generated by the sample). The intracellular deoxyhemoglobin produces stronger magnetic fields than those generated in the deoxyhemoglobin-free extracellular space. This heterogeneity of magnetic field strength within the sample leads to the presence of local magnetic gradients between the intra- and extracellular spaces, resulting in rapid dephasing (short T2) of protons that freely diffuse across the cell membrane [5, 20–22].

This hypothesis receives strong support from two independent sources. First, it has recently been demonstrated that the hypointensity within hematomas is seen more commonly and extensively with gradient-echo pulse sequences than with long TR/long TE SE pulse sequences [21]. Gradient-echo scans are more sensitive to magnetic susceptibility effects because they are more dependent on T2* than on T2. Second, magnetic susceptibility effects of deoxyhemoglobin have been demonstrated in vitro with MR spectroscopy, even before the development of MR imaging [16, 20].

With MR spectroscopy, the degree of T2 shortening is proportional to the square of both the hemoglobin concentration and the magnetic field strength [20, 22]. The in vitro data help to explain some of the phenomena encountered in our clinical cases, but in other important ways are at variance with clinical experience. The dependence of intensity on the square of the deoxyhemoglobin concentration is probably the cause of the variability of intensity (both within an individual hematoma and between hematomas) as well as the rapid changes in intensity that occur over time. Unfortunately, the intensity patterns encountered at 0.5 T do not match those predicted by in vitro data. Hypoxic, intact RBCs are located at the center of hematomas, and thus central hypointensity should be the commonly encountered pattern [5]. In our experience, however, hypointense foci are often located eccentrically (Fig. 4), and, as previously stated, a thin rim of hypointensity is seen at the margin of many clots (Figs. 2, 4, and 5). The eccentric location of the hypointense focus may reflect areas of recurrent hemorrhage (Fig. 4); one of the striking features in our series was the evidence of clinically silent rehemorrhage (as documented by serial CT and/or MR studies demonstrating increase in hematoma size) in six cases. Given the apparent sensitivity of clot intensity to deoxyhemoglobin concentration, even minimal rehemorrhage might significantly alter the intensity of the hematoma.

The hypointense peripheral rim is more puzzling. This phenomenon has been described in chronic hemorrhage, where it is said to reflect a magnetic susceptibility effect of hemosiderin within macrophages in the capsule of aging hematomas [5]. The hypointense rim in acute hematomas is less prominent but otherwise similar in appearance. At this stage of hematoma evolution, hemosiderin-laden macrophages are not present [23–25]; thus, another explanation for this phenomenon must be sought. Edelman et al. [21] noted this hypointense rim and suggested that it might represent a border-zone phase-shift phenomenon. In our experience, similar rims have also been seen at the margin of all abscesses and some metastatic foci [26, 27]. Pathologic studies in these cases have demonstrated the presence of macrophages, but without hemosiderin. We believe that this represents a paramagnetic effect of free radicals produced by macrophages during active phagocytosis [27] and believe it may account for the rim hypointensity encountered in acute hematomas as well.

A far more striking and troubling discrepancy between predictions based on in vitro MR spectroscopy and clinical data is the dependence of magnetic susceptibility on the square of the field strength of the MR unit [20, 22]. This led Gomori et al. [5] to state that hypointensity would be seen only at high field strengths (1.5 T). This is clearly not the case in clinical practice. Hypointensity is routinely seen on intermediate-field-strength systems (0.35–0.6 T), as demonstrated by us (Figs. 3–5) and in other publications [8, 12, 18, 21], even though magnetic susceptibility is theoretically one-ninth that seen at 1.5 T. More surprisingly, acute hematomas studied at 0.15 T (magnetic susceptibility 1/100 that seen at 1.5 T) and even at 0.02 T (magnetic susceptibility 1/5625 that seen at 1.5 T) also demonstrate mild hypointensity (see Fig. 2E of Sipponen et al. [1], Fig. 2C of DeLaPaz et al. [3], and Figs. 1B and 6C of Sipponen et al. [4]). Based on a comparison of published images, it appears that the degree of hypointensity does indeed vary with field strength, but to a lesser extent than that predicted by in vitro studies. The discrepancy between experimental prediction and clinical observation should not come as a complete surprise, given the complexity of hemorrhagic brain lesions. Reactive changes within and/or adjacent to hematomas could modify the intensities encountered on clinical images. Additional factors, un-

affected by field strength, could thus contribute to the development of hypointensity at low fields or militate against full expression of hypointensity at high field strengths, lessening the dependence of intensity on field strength.

The next major change in hematoma intensity on long TR scans is the redevelopment of hyperintensity (Figs. 4 and 5), which begins on approximately the fourth postictal day. (This reversal of intensity may occur quickly; that is, in 24–48 hr.) Thus, hematomas pass through a second isointense phase (Fig. 6) to become hyperintense relative to brain by the end of the first week. The redevelopment of hyperintensity is a result of RBC lysis. The overall deoxyhemoglobin concentration decreases and deoxyhemoglobin becomes homogeneously distributed in the extracellular space. This eliminates the heterogeneous magnetic field, and thus local magnetic gradients within the sample disappear. The increased intensity, therefore, results from a simple subtraction of the T2 shortening effect of the intracellular deoxyhemoglobin; the intrinsically prolonged T2 of blood is unmasked and the intensity returns to its initial high level. Additional prolongation of T2 during this period may result from an increase in water within the hematoma as cells lyse and the clots age [23, 24]. It is important to remember that the increase in intensity that occurs on long TR scans during this period is not caused by the presence of methemoglobin, which produces the nearly simultaneous increase in intensity seen on short TR scans. The paramagnetic effect of methemoglobin produces marked T1 and, to a lesser extent, T2 shortening. On long TR scans, all intracranial soft tissues have undergone complete interpulse recovery; thus, a decrease in T1 does not increase the intensity of the hemorrhage relative to brain. The T2 shortening effect of methemoglobin should actually cause diminished signal intensity, but this effect is obviously overcome by more powerful determinants of T2. High proton density may also contribute to the increased intensity encountered on long TR scans at this stage, especially when used in conjunction with a short or intermediate TE.

In addition to these already complex phenomena, two additional factors significantly affect hematoma intensity. The first factor is recurrent hemorrhage, which is extremely difficult to diagnose in any individual case because rapid intensity changes occur with (Fig. 4) or without (Fig. 5) rehemorrhage. In general, rehemorrhage appears to be a major source of the heterogeneity and variability of hematoma intensity. The admixture of extravasated blood of various ages probably accounts for the almost random pattern of heterogeneous intensity encountered within recurrent hemorrhages (Fig. 4). The presence of unsuspected preexisting hemorrhage and the development of postictal rehemorrhage explain, at least in part, the overall variations in intensity encountered among different patients. For instance, MR performed in an elderly patient 60 hr after the onset of mild hemiparesis and obtundation demonstrated a large subdural hematoma that was "prematurely" hyperintense on short TR/short TE scans. It is most likely, given the patient's clinical and CT findings, that this was a rehemorrhage into a clinically silent chronic subdural hematoma. Postictal rehemorrhage may account for the persistence of hypointensity on long TR scans into the sixth and seventh days in five of the examples of rehemorrhage evaluated in our series (Fig. 4F).

The other source of intensity variation is the location of the hematoma. When time/intensity relationships for AIH in different intracranial compartments were studied, no clear trends were discerned, but, when scans demonstrating hemorrhage into multiple compartments were evaluated, it was noted that the intensities were different in nine of 12 cases. This difference was most marked when hemorrhage into a spinal fluid compartment (intraventricular or subarachnoid) was seen in conjunction with either a parenchymal or extraaxial hematoma (Fig. 3). Subarachnoid hemorrhage was particularly difficult to detect on MR. Acute (under 3 days) and/or diffuse subarachnoid hemorrhage could not be detected (Fig. 3C). This poor visualization of diffuse subarachnoid hemorrhage has already been noted [3, 13]. Some investigators have ascribed it to the higher oxygen tension of CSF when compared with brain, which leads to a low deoxyhemoglobin concentration [28, 29]. In the absence of deoxyhemoglobin, T2 shortening and hypointensity do not develop during the acute posthemorrhage period. Another factor that may contribute to the poor visualization of diffuse subarachnoid hemorrhage is the effect of spinal fluid pulsation on observed intensity. Recent studies indicate phase-shift effects of spinal fluid pulsation may contribute significantly to the observed intensity within spinal fluid spaces [30]; therefore, it is possible that the effects of hemorrhage on spinal fluid intensity might be masked.

In summary, the complexity of the intensities encountered in AIH is a true reflection of the complex biochemical changes that occur during the first posthemorrhagic week. These changes are clearly interdependent, but the extent to which each occurs, the timing of the occurrence, and the location within an individual hematoma vary. The overall intensity and/or specific intensity pattern encountered within any individual hematoma will, therefore, reflect the nearly unique interplay of these factors at one particular moment. Under these circumstances, the variable, heterogeneous, and somewhat unpredictable appearance of these lesions is to be expected.

Since a wide range of intensities are encountered in AIH, it is obvious that no single sequence and no single intensity can characterize acute hemorrhage. It is, however, possible to define characteristic (although not necessarily specific) combinations of intensities on multiple-pulse sequences at four different stages of AIH evolution:

Stage I (under 24 hr)—subtle hyperintensity on short TR/short TE scans and moderate to marked hyperintensity on long TR/intermediate TE and long TR/long TE scans, respectively (Fig. 2). This combination is relatively specific (especially when a thin, hypointense rim is also present), since most lesions hyperintense on long TR scans are hypo- to isointense on short TR scans.

Stage II (1–3 days)—iso- to mild hypointensity on short TR/short TE scans and marked hypointensity on long TR/intermediate to long TE scans (Figs. 3–5). Although characteristic, this pattern is not as specific as previously suggested [5]. Marked hypointensity may also be encountered in densely calcified lesions [31] and noncalcified nonhemorrhagic granulomatous masses [26, 32, 33].

Stage III (4–6 days)—hyperintensity on short TR/short TE images and markedly variable intensity on long TR/interme-

diate to long TE scans. When marked hypo- or hyperintensity are present on long TR scans, hemorrhage may be diagnosed with confidence; however, if scans are obtained just as intensity is beginning to increase on long TR scans, findings may be indistinguishable from those seen in fat-containing lesions (Fig. 6).

Stage IV (more than 6–7 days)—hyperintensity on short TR/short TE and long TR/intermediate-to-long TE scans. This combination is considered specific, but it may be encountered rarely in intracranial dermoids [34].

The ability to detect and characterize hematomas is dependent on anatomy as well as intensity; therefore, the degree to which a lesion distorts normal anatomy also has a significant effect on hematoma detection. Subarachnoid hemorrhage is difficult to visualize on MR, not only because it fails to alter intensity, but also because it fails to produce anatomic distortion (Fig. 3). Parenchymal hematomas (Fig. 2) are always detected on MR, but they may be difficult to specifically characterize as hemorrhagic lesions; conversely, extraaxial hematomas (subdural and epidural, Figs. 2 and 3) have characteristic and relatively specific anatomic configurations that make the diagnosis of hematoma possible regardless of intensity. In fact, because of the absence of bone artifacts and the excellent contrast between brain and adjacent spinal fluid, small, extraaxial hematomas are detected much more easily on MR than on CT (Fig. 2) [6, 35].

In conclusion, the complex nature of the intensity changes encountered in acute intracranial hemorrhage and the difficulty in distinguishing some of these changes from those seen in other lesions suggest that CT will remain the procedure of choice as the screening test in the evaluation of any patient suspected of acute intracranial hemorrhage. Once the hemorrhagic nature of the lesion is identified on CT, MR can be used to increase diagnostic information by more accurately demonstrating the extent of the abnormality, assessing the time from hemorrhage, and detecting the presence of underlying lesions.

REFERENCES

1. Sipponen JT, Sepponen RE, Sivula A. Nuclear magnetic resonance (NMR) imaging of intracerebral hemorrhage in the acute and resolving phases. *J Comput Assist Tomogr* **1983**;7:954–959
2. Han JS, Kaufman B, Alfidi RJ, et al. Head trauma evaluated by magnetic resonance and computed tomography: a comparison. *Radiology* **1984**; 150:71–77
3. DeLaPaz RL, New PF, Buonanno J, et al. NMR imaging of intracranial hemorrhage. *J Comput Assist Tomogr* **1984**;8:599–607
4. Sipponen JT, Sepponen RE, Tanttu JI, Sivula A. Intracranial hematomas studied by MR imaging at 0.17 and 0.02T. *J Comput Assist Tomogr* **1985**;9:698–704
5. Gomori JM, Grossman RI, Goldberg HI, Zimmerman RA, Bilaniuk LT. Intracranial hematomas: imaging by high field MR. *Radiology* **1985**; 157:87–93
6. Snow RB, Zimmerman RD, Gandy SE, Deck MDF. Comparison of magnetic resonance imaging and computed tomography in the evaluation of head injury. *Neurosurgery* **1986**;18:45–52
7. Dooms GC, Uske A, Brant-Zawadzki M, et al. Spin echo MR imaging of intracranial hemorrhage. *Neuroradiology* **1986**;28:132–138
8. Zimmerman RD, Deck MDF. Intracranial hematomas: imaging by high field MR. *Radiology* **1986**;159:565
9. Zimmerman RA, Bilaniuk LT, Grossman RI, et al. Resistive NMR of intracranial hematomas. *Neuroradiology* **1985**;27:16–20
10. New PF, Aronow S. Attenuation measurements of whole blood and blood fractions in computed tomography. *Radiology* **1976**;121:635–640
11. Scotti G, Terbrugge K, Melancon D, et al. Evaluation of the age of subdural hematomas by computerized tomography. *J Neurosurg* **1977**;47:311–315
12. Di Chiro G, Brooks RA, Girton ME, et al. Sequential MR studies of intracerebral hematomas in monkeys. *AJNR* **1986**;7:193–199
13. Chakeres DW, Bryan RN. Acute subarachnoid hemorrhage: in vitro comparison of magnetic resonance and computed tomography. *AJNR* **1986**;7:223–228
14. Bydder GM, Magnetic resonance imaging of the brain. *Radiol Clin North Am* **1984**;22:779–794
15. Wehrli FW, MacFall JR, Shutts P, Breger R, Herfkens RJ. Mechanisms of contrast and NMR imaging. *J Comput Assist Tomogr* **1984**;8:369–380
16. Brooks RA, Battocletti JH, Sances A, et al. Nuclear magnetic relaxation in blood. *IEEE Trans Biomed Eng* **1975**;22:12–18
17. Bradley WG, Schmidt PG. Effect of methemoglobin formation on the MR appearance of subarachnoid hemorrhage. *Radiology* **1985**;156:99–103
18. Harms SE, Siemers PT, Hildenbrand T, Plum G. Multiple spin echo magnetic resonance imaging of the brain. *Radiographics* **1986**;6:117–134
19. Wolf GL, Burnett KR, Goldstein EJ, Joseph PM. Contrast agents for magnetic resonance imaging. In: Kressel HY, ed. *Magnetic resonance annual 1985*. New York: Raven, **1985**:231–266
20. Brittenham GM, Farrell DE, Harris JW, et al. Magnetic susceptibility measurements of human iron stores. *N Engl J Med* **1982**;307:1671–1675
21. Edelman RR, Johnson K, Buxton R, et al. MR of hemorrhage: a new approach. *AJNR* **1986**;7:751–756
22. Thulborn KR, Waterton JC, Matthews PM, Radda GK. Oxygenation dependance of the transverse relaxation time of water protons in whole blood at high fields. *Biochim Biophys Acta* **1982**;174:265–270
23. Stehbens WE. Intracerebral and intraventricular hemorrhage. In: *Pathology of cerebral blood vessel*. Saint Louis: Mosby, **1972**:284–350
24. Adams RD, Sidman RL. *Introduction of neuropathology*. New York: McGraw Hill, **1968**:177–178
25. Lindenberg R. Pathology of craniocerebral injuries. In: Newton TH, Potts DE, eds. *Radiology of the skull and brain, vol 3. Anatomy and pathology*. Saint Louis: Mosby, **1977**:3049–3087
26. Zimmerman RD, Becker RD, Devinsky O, et al. MRI features of cerebral abscesses and other intracranial inflammatory lesions (excluding AIDS patients). Presented at the Symposium Neuroradiologicum, Stockholm, June **1986**
27. Fleming CA, Zimmerman RD, Becker RD, Deck MDF. The diagnostic significance of rim intensity and edema patterns in the differentiation of intracranial mass lesions on MRI. Presented at the annual meeting of the American Society of Neuroradiology, New York City, May **1987**
28. Kemp SS, Grossman RI, Ip CY, et al. The importance of oxygenation in the appearance of acute subarachnoid hemorrhage on high field magnetic resonance imaging. Presented at Symposium Neuroradiologicum, Stockholm, June **1986**
29. Gomori JM, Grossman RI. Mechanisms responsible for the MR appearance and evolution of intracranial hemorrhage. *Radiology* **1986**;161(P):364
30. Rubin JB, Enzmann DR. Imaging spinal CSF pulsation by 2DFT magnetic resonance: significance during clinical imaging. Harmonic modulation of proton MR precessional phase by pulsatile motion: origin of spinal CSF flow phenomenon. Presented at the annual meeting of the American Society of Neuroradiology, San Diego, January **1986**
31. Oot RF, New PF, Pile-Spellman J, et al. Detection of intracranial calcifications by MR. *AJNR* **1986**;7:801–810
32. Becker RD, Zimmerman RD, Sze G, Haimes AB, Deck MDF. MR of subdural empyema and other extra-axial inflammatory lesions. Presented at the annual meeting of the American Society of Neuroradiology, New York City, May **1987**
33. Sherman JL, Hayes WS, Stern BJ, Citrin CM, Pulaski PD. MR evaluation of intracranial sarcoidosis: comparison with CT. Presented at the annual meeting of the American Society of Neuroradiology, New York City, May **1987**
34. Newton DR, Larson TC, Dillon WP, Newton TH. Magnetic resonance characteristics of cranial epidermoid, dermoid and teratomatous tumors. Presented at the annual meeting of the American Society of Neuroradiology, New York City, May **1987**
35. Zimmerman RD, Snow RB, Gandy SE, et al. Comparison of MRI and CT in the evaluation of head trauma: review of initial 100 cases. Presented at the Symposium Neuroradiologicum, Stockholm, June **1986**

This article has been cited by:

1. Toshio Moritani, Akio Hiwatashi, Sravanthi Koduri, Zachary Marcus Wilseck, Ankur Bhambri, Aditya S. Pandey. Intracranial Hemorrhage 187-216. [Crossref]
2. Josep Brocal, Roberto José López, Gawain Hammond, Rodrigo Gutierrez-Quintana. 2017. Intracerebral haemorrhage in a dog with steroid-responsive meningitis arteritis. *Veterinary Record Case Reports* **5**:1. . [Crossref]
3. Jimo Jeong, Sangjun Park, Eunseok Jeong, Namsoo Kim, Minsu Kim, Yechan Jung, Youngkwon Cho, Kichang Lee. 2016. Time-dependent low-field MRI characteristics of canine blood: an in vitro study. *Journal of Veterinary Science* **17**:1, 103. [Crossref]
4. Julius Griauzde, Elliot Dickerson, Joseph J. Gemmete. Hemorrhagic Stroke 383-412. [Crossref]
5. J. Jacob Kazam, Apostolos John Tsiouris. 2015. Brain Magnetic Resonance Imaging for Traumatic Brain Injury. *Topics in Magnetic Resonance Imaging* **24**:5, 225-239. [Crossref]
6. Yi Wang, Tian Liu. 2015. Quantitative susceptibility mapping (QSM): Decoding MRI data for a tissue magnetic biomarker. *Magnetic Resonance in Medicine* **73**:1, 82-101. [Crossref]
7. Julius Griauzde, Elliot Dickerson, Joseph J. Gemmete. Hemorrhagic Stroke 1-34. [Crossref]
8. Allyson R. Zazulia, Michael N. Diringer. Nontraumatic Intracerebral and Subarachnoid Hemorrhage 191-202. [Crossref]
9. John J. Wasenko, Leo Hochhauser. Central Nervous System Trauma 295-335. [Crossref]
10. A. Hiwatashi. Intracranial Hemorrhage 75-92. [Crossref]
11. T. Sugawara, A. Wang, V. Jadhav, T. Tsubokawa, A. Obenaus, John H. Zhang. Magnetic resonance imaging in the canine double-haemorrhage subarachnoid haemorrhage model 235-239. [Crossref]
12. Jane M. Hawnaur, Ian Isherwood. MRI at Midfield Strength . [Crossref]
13. Kostas N. Fountas, Eftychia Z. Kapsalaki, Joe Sam Robinson. 2006. Cervical epidural hematoma in children: a rare clinical entity. *Neurosurgical Focus* **20**:2, 1-4. [Crossref]
14. Masato KITAGAWA, Midori OKADA, Kiichi KANAYAMA, Takeo SAKAI. 2005. Traumatic Intracerebral Hematoma in a Dog: MR Images and Clinical Findings. *Journal of Veterinary Medical Science* **67**:8, 843-846. [Crossref]
15. Thomas Allkemper, Bernd Tombach, Wolfram Schwindt, Harald Kugel, Matthias Schilling, Otfried Debus, F. Möllmann, Walter Heindel. 2004. Acute and Subacute Intracerebral Hemorrhages: Comparison of MR Imaging at 1.5 and 3.0 T—Initial Experience. *Radiology* **232**:3, 874-881. [Crossref]
16. M. Alemany Ripoll, O. Gustafsson, B. Siosteen, Y. Olsson, R. Raininko. 2002. MR follow-up of small experimental intracranial haemorrhages from hyperacute to subacute phase. *Acta Radiologica* **43**:1, 2-9. [Crossref]
17. Veit Rohde, Ina Rohde, Ruth Thiex, Wilhelm Küker, Azize Ince, Joachim Michael Gilsbach. 2001. The role of intraoperative magnetic resonance imaging for the detection of hemorrhagic complications during surgery for intracerebral lesions an experimental approach. *Surgical Neurology* **56**:4, 266-274. [Crossref]
18. Annette J. Johnson, Daniel K. Kido, William D. Shannon, Mark M. Bahn, Mokhtar H. Gado, Benjamin C. P. Lee, Christopher J. Moran, Franz J. Wippold, Benjamin Littenberg. 2001. Evaluation of a Reduced MR Imaging Sequencing Protocol in Adult Patients with Stroke. *Radiology* **218**:3, 791-797. [Crossref]
19. Lisa S. Klopp, John T. Hathcock, Donald C. Sorjonen. 2000. MAGNETIC RESONANCE IMAGING FEATURES OF BRAIN STEM ABSCESSATION IN TWO CATS. *Veterinary Radiology <html_ent glyph="@amp;" ascii="&"/> Ultrasound* **41**:4, 300-307. [Crossref]
20. Tomonori TAMAKI, Ichirou TAKUMI, Takayuki KITAMURA, R. Yoshiyuki OSAMURA, Akira TERAMOTO. 2000. Pituitary Stone. Case Report. *Neurologia medico-chirurgica* **40**:7, 383-386. [Crossref]
21. M. Reither. Zentralnervensystem (ZNS) und Spinalkanal 43-124. [Crossref]
22. Alison E. Baird, Steven Warach. 1998. Magnetic Resonance Imaging of Acute Stroke. *Journal of Cerebral Blood Flow & Metabolism* **18**:6, 583-609. [Crossref]
23. James V. Byrne, Guido Guglielmi. Imaging for Intracranial Aneurysms 75-102. [Crossref]
24. M. R. Patel, R. R. Edelman, S. Warach. 1996. Detection of Hyperacute Primary Intraparenchymal Hemorrhage by Magnetic Resonance Imaging. *Stroke* **27**:12, 2321-2324. [Crossref]
25. D. B. Mikkelsen. 1996. Lumbar Disk Herniation Combined with Epidural Hematoma. *Acta Radiologica* **37**:1P1, 145-147. [Crossref]

26. Bernard H. Bochner, Seth P. Lerner, Mark Kawachi, Richard D. Williams, Peter T. Scardino, Donald G. Skinner. 1995. Postradical orchiectomy hemorrhage: Should an alteration in staging strategy for testicular cancer be considered?. *Urology* **46**:3, 408-411. [Crossref]

27. G. Guizar-Sahagun, F. Rivera, E. Babinski, E. Berlanga, M. Madrazo, R. Franco-Bourland, I. Grijalva, J. Gonzalez, B. Contreras, I. Madrazo. 1994. Magnetic resonance imaging of the normal and chronically injured adult rat spinal cord in vivo. *Neuroradiology* **36**:6, 448-452. [Crossref]

28. T. A. Sweasey, J. A. Brunberg, P. E. McKeever, H. M. Sandler, W. F. Chandler. 1994. Cystic Cervical Intramedullary Ependymoma with Previous lntracyst Hemorrhage: Magnetic Resonance Imaging at 1.5 T. *Journal of Neuroimaging* **4**:2, 111-113. [Crossref]

29. M. Mascalchi, G. Dal Pozzo, C. Dini, V. Zampa, M. D'andrea, M. Mizzau, F. Lolli, D. Caramella, C. Bartolozzi. 1993. Acute spinal trauma: Prognostic value of MRI appearances at 0.5 T. *Clinical Radiology* **48**:2, 100-108. [Crossref]

30. F. Triulzi. 1990. Cerebral Hemorrhage: CT and MRI. *Rivista di Neuroradiologia* **3**:2_suppl, 39-44. [Crossref]

31. Douglas J. Quint, Eric M. Spickler. 1990. Magnetic resonance demonstration of vertebral artery dissection. *Journal of Neurosurgery* **72**:6, 964-967. [Crossref]

32. Ziad L. Deeb, William E. Rothfus, Andrew L. Goldberg, Richard H. Daffner. 1990. Absent cord sign in acute spinal trauma. *Clinical Imaging* **14**:2, 138-142. [Crossref]

33. S. Cirillo, F. Di Salle, L. Simonetti, R. Spaziante, R. Elefante, F. Smaltino. 1989. La risonanza magnetica nell'emorragia subaracnoidea. *Rivista di Neuroradiologia* **2**:3, 211-217. [Crossref]

34. S. Cirillo, L. Simonetti, F. Di Salle, L. Stella, R. Elefante, F. Smaltino. 1989. La risonanza magnetica nell'emorragia subaracnoidea. *Rivista di Neuroradiologia* **2**:3, 219-225. [Crossref]

35. . Intracranial Hemorrhage 55-71. [Crossref]